Sweet Solution for Sticky Problems: Chemoreological Design of Self-Adhesive Gel Materials Derived From Lipid Biofeedstocks and Adhesion Tailoring via Incorporation of Isosorbide

ARTICLE *in* MACROMOLECULES · MAY 2013

Impact Factor: 5.8 · DOI: 10.1021/ma400203v

2 AUTHORS:

Richard Vendamme
Nitto Denko Corporation, Belgium, Genk
24 PUBLICATIONS **285** CITATIONS
SEE PROFILE

Walter Eevers
Flemish Institute for Technological Research
31 PUBLICATIONS **112** CITATIONS
SEE PROFILE

Macromolecules

Article

pubs.acs.org/Macromolecules

Sweet Solution for Sticky Problems: Chemoreological Design of Self-Adhesive Gel Materials Derived From Lipid Biofeedstocks and Adhesion Tailoring via Incorporation of Isosorbide

Richard Vendamme*[,†] and Walter Eevers[†,‡]

[†]Nitto Europe N.V., 22 Eikelaarstraat, 3600 Genk, Belgium

[‡]Nitto Denko Europe Technical Centre Sarl, Quartier de l'Innovation de L'EPFL, Bâtiment G, 1015 Lausanne, Switzerland

Supporting Information

ABSTRACT: This article describes the synthesis of functional pressure-sensitive adhesives (PSA) derived from plant oils and highlights how the viscoelastic and adhesion properties can be tailored by incorporation of the cereal-based monomer 1,4:3,6-dianhydro-D-glucitol (isosorbide). At first, the synthesis of carboxylic acid-terminated polyesters from bulk polycondensation of dimerized fatty acids with several diols such as dimer fatty diol, butanediol or isosorbide is described. The resulting polymers were then fully characterized, before being cured with epoxidized plant oils to form viscoelastic bioelastomers with tunable stickiness degrees. The role of isosorbide in the rheological and adhesion profiles of the glues was investigated and discussed. These renewable coatings combined the intrinsic flexibility of lipids with the polarity of sugars and demonstrate interesting performances. This article exemplifies that in soft materials such as PSA, isosorbide can play multiple roles such as adjusting the glass transition temperature, modulating the viscoelastic spectrum, and tuning the interfacial properties of the glue, and this gives a new twist to this promising renewable monomer that, up to now, has mostly been incorporated in rigid polymeric systems.

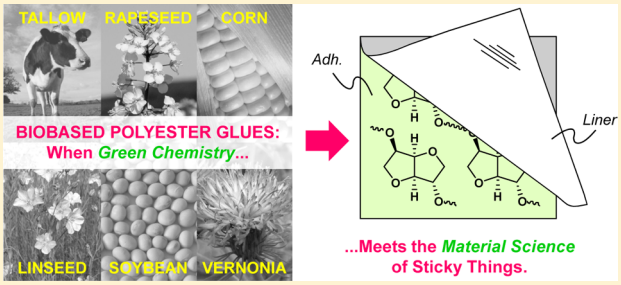

INTRODUCTION

It is now widely accepted that the petroleum-based economical era will only be a brief interlude in the history of humankind and that, in the long term, the chemical and adhesive industries will have to invent more sustainable models integrating the renewability of their energetic and raw material resources as prerequisite elements. In this framework, the use of raw materials derived from biomass is rapidly increasing,[1−3] because the availability of cheap fossil raw materials has already a foreseeable limit as crude oil is being depleted. The development of economically viable biobased materials and coatings yielding the proper product functions required in the current highly specific applications can be seen as a robust foundation for the emergence of a new biobased economy.[4]

Pressure sensitive adhesive (PSA) materials are a peculiar class of glues intended to form a reversible bond simply by the application of a light pressure to marry the adhesive with the adherent.[5−7] Conceptually, PSAs must be designed with a subtle balance between flow and resistance to flow: the bond forms because the adhesive is soft enough to wet the adherent, but the bond also has suitable strength because the adhesive is cohesive enough to resist the stress of the debonding stage. In practice, the formation, development, and strength of the adhesive bonds can be tuned by thoughtfully adjusting the bulk viscoelastic properties of the glue and by incorporating functional monomers within the base−polymer structure.[8] To date, important families of polymers for PSA applications belong either to acrylic copolymers, natural rubber, styrene−isoprene−styrene (SIS) block copolymers, styrene−butadiene−styrene (SBS) block copolymers, styrene−butadiene rubber (SBR), and polysiloxanes. In addition to these well-established chemical families, polyesters are recently emerging as a viable and sustainable alternative for pressure sensitive adhesion.[9,10] Most commercial PSA are still based on petroleum resources (except natural rubber) and there is a pressing need to develop more sustainable PSA chemistries.

Fatty acid derivatives are an attractive resource for the development of biobased adhesives because of their intrinsically low glass transition temperature and the wide-range of chemical and biorefining operations available for triglyceride plant oils.[11,12] For instance, the synthesis of renewable PSA via photocatalyzed cationic polymerization of epoxidized soybean oil (ESO) has been disclosed in a recent patent application.[13] In addition, Sun et al. proposed an inspiring concept of renewable PSA derived from ESO and dihydroxyl soybean oil without using any petrochemicals,[14] and Wool reported the design of biobased PSA from acrylated methyl oleate.[15,16]

Received: January 29, 2013
Revised: April 12, 2013
Published: April 23, 2013

Table 1. Biobased Co- and Ter-Polyesters Synthesized from Dimerized Fatty Acids Pripol 1009 (P1009)[a], Pripol 1006 (P1006),[a] and Pripol 1040 (P1040)[a] in Combination with Pripol 2033 (P2033), Butane Diol (BDO), or Isosorbide (IS)

		molar ratios[b]		polymer characteristics				
entry	feed composition (g): P1009/P1006/P1040•P2033/BDO/IS	Φ	Ψ (μmol/g)	T_g[c] (°C)	M_w (g/mol)	PDI	AV (mg KOH/g)	OHV (mg KOH/g)
		Aliphatic Polyesters						
P1	179.46/−/−•145.54/−/−	0.540	12.07	−46.3	23 334	2.39	14.84	0.05
P2	185.96/−/−•139.04/−/−	0.560	12.06	−46.5	13 409	2.31	22.32	0.01
P3	178.31/−/7.63•139.06/−/−	0.560	33.1	−46.8	16 232	2.42	22.74	0.03
P4	162.18/−/23.76•139.07/−/−	0.560	77.62	−46.7	20 644	2.83	22.21	0.02
P5	184.87/−/7.58•132.55/−/−	0.580	32.96	−46.6	12 653	2.41	30.67	0.01
P6	−/276.60/6.91•−/41.49/−	0.522	29.25	−46.5	18 701	2.76	20.84	0.12
		Isosorbide-Based Polyesters						
Pi1	−/ 261.21/−•−/−/63.79	0.514	28.43	−18.2	27 032	2.57	13.52	2.89
Pi2	−/ 263.37/−•−/−/61.63	0.525	28.69	−18.6	14 221	2.61	22.48	1.81

[a]P1009 is a pure dimer fatty acid containing less than 1% of trimer, P1006 is a slightly more functional dimer (3% of trimer), and P1040 is a trimer with 20% of trimer. [b]Φ = [COOH]/([COOH]+[OH]) is the molar ratio of functional groups introduced in the reaction vessel; Ψ is the amount of trifunctional monomers introduced in the reactor (expressed in μmol trimer/g polymer). [c]Glass transition temperature determined from the G'' maxima in DMA in the second heating ramp at +2 °C/min.

Besides plant oils, polysaccharides[17] and sugar-based[18,19] building blocks also represent an attractive resource for the design of biobased PSA, due to their high degree of functionality, low cost, and biodegradability. In that respect, 1,4:3,6-dianhydro-D-glucitol (commonly known as isosorbide) is an interesting and commercially available diol derived from starch via its synthetic intermediate sorbitol.[20] A huge body of work exists describing the use of isosorbide (IS) as a renewable building block for the synthesis of functional polymers.[21−23] But although the incorporation of IS in rigid polymer systems with high glass transition temperatures (T_g) has been extensively studied, there is no study addressing its potential utility in soft and/or sticky materials, to the best of our knowledge.

We anticipated that low T_g polyesters synthesized from a combination of lipid-based and sugar-based monomers would combine the intrinsic properties of their precursors such as softness, flexibility and polarity, and therefore could form the basis of a new class of renewable and functional bioadhesive gel materials. The logic of this article articulates itself around three objectives: (i) in the first part, we describe the synthesis and characterization of carboxylic acid-terminated renewable polyesters from bulk polycondensation of dimerized fatty acids with several diols such as dimer fatty diol, butanediol or IS. (ii) in a second step, we demonstrate how these polyesters can be cross-linked with epoxidized plant oils to form viscoelastic elastomers with various degrees of stickiness; (iii) finally, adhesion characteristics of the coating were investigated, and the role of IS in the rheological and adhesion profiles of the glues was discussed.

EXPERIMENTAL SECTION

Materials. High purity IS (99.5%+) was obtained from Roquette Frères (Lestrem, France) under the trade name Polysorb P. The fully hydrogenated dimer fatty acid (Pripol 1009 and/or Pripol 1006) and dimer fatty diol (Pripol 2033) were supplied from Croda (Gouda, The Netherlands). A mixture containing 20% of dimerized fatty acids and 80% of trimerized fatty acids was equally obtained from Croda (Pripol 1040). Titanium tetrabutoxide (Ti[OBu]$_4$) and 1,4-butanediol were purchased from Sigma-Aldrich. Epoxidized linseed oil (ELO) and epoxidized soybean oil (ESO) were obtained from Cognis (Düsseldorf, Germany) under the trade name Dehysol B376 Spezial and Dehysol D82, respectively. Refined Vernonia Galamensis Oil (VGO) was obtained from Dr. Robert E. Perdue, former head of Vertech Inc. (Plano, Texas). The catalyst for the epoxy-carboxy curing reaction (Nacure XC-9206) was supplied from King Industries, Inc. (Norwalk, Connecticut). All chemicals were used as received without further purification.

Polycondensation. Polymer Pi1 was synthesized according to the following protocol. Pripol 1009 (261.21g, 460.8 mmol) and IS (63.79g, 436.49 mmol) were weighed into a 1L round-bottom glass flange reactor. The reactor was fitted with a dean-stark apparatus mounted with an Allihn condenser and a digital overhead stirrer. During the first part of the synthesis, the setup was continuously flushed with nitrogen to prevent oxidation and facilitate transport of the condensation byproduct (water). While stirring, the mixture was heated to 180 °C overnight using an electromantle connected with a temperature controller. The temperature was then increased to 200 °C and vacuum processing (2 to 4 mbar) was applied for 30 min. Vacuum processing was briefly interrupted and titanium tetrabutoxide (0,02 mol % relative to the carboxylic acid functions) dissolved in xylene was added to the melt. The reaction was continued under vacuum with incremental temperature steps at 220 °C, 235 °C and finally 250 °C (2 h for each step). The polymer was finally cooled down to 100 °C and discharged from the reactor as a clear transparent honey-like substance. All polymers were prepared according to similar procedures. Compositions and properties of the synthesized polymers are given in Table 1.

Analytics. The average molecular weights of the fatty acid based polymers were determined by gel permeation chromatography (GPC) instrument (Waters Model Pump 515 and Waters 2414 refractive index detector) with Styragel columns relative to polystyrene (PS) standards using tetrahydrofuran (THF) as eluent. Fourier transform infrared spectroscopy (FTIR) analysis of the polyester adhesives was performed using a Thermo Scientific Nicolet 8700 spectrometer. The acid and hydroxyl values of the polymers were monitored via standard titration methods as previously described.[10] Epoxy values of the cross-linkers were titrated according to the standard pyridine/HCl method.

Formulation, Coating, and Curing. Predetermined amounts of COOH-terminated polyesters, epoxy plant oil and catalyst (Nacure XC-9206) are weighed with a microbalance, and homogenized with a small amount of ethyl acetate (the solid base of the formulations was fixed at 70 wt %, i.e. 30 wt % of solvent). The adhesive formulations are always designated by the codes Pα-β%δ, where Pα refers to the base polymer (see Table 1), β corresponds to the wt % of epoxy plant oil (relative to the weight of base polymer Pα), and δ refers to the catalyst wt % (relative to the total formulation weight). Coating and curing of the resin were made by manual roll-coating of the reactive solutions with an approximate speed of 5 cm/s on a 50 μm thick polyethylene terephtalate (PET) base film. This bilayer stack was

dx.doi.org/10.1021/ma400203v | Macromolecules 2013, 46, 3395−3405

cured in a thermal oven at 155 °C during 45 min. Dry thickness of glue layers was 20 ± 1 μm. After curing, the adhesive surfaces were covered with an antiadhesive siliconized paper.

Dialysis. Around 0.15 g of a cured adhesive coated on a siliconized PET film were packed into a sealed pocket made of a folded, porous PTFE membrane (Temish membrane from Nitto Denko Corporation). After 2 weeks of immersion in a large excess of toluene, the dialysis bag was removed and dried. The gel content (gel %) was determined gravimetrically from the average of two measurements. The sample weight after dialysis refers to the insoluble gel fraction, whether the difference between the initial and dialyzed weights corresponds to the sol fraction of the networks.

Rheology. For all the rheological investigations, reactive formulations containing the polymer, epoxy oil, and curing catalyst were prepared without solvent and homogenized at 70 °C for 20 min under manual stirring. The air bubbles introduced by the mixing process were removed by centrifugation. Curing kinetics of the adhesive resins was monitored with an AR 1000 rheometer (TA Instruments) in parallel plate geometry (20 mm diameter and 0.6 mm gap) in dynamic mode with a strain of 0.01 within the linear viscoelastic regime (i.e., with G' and G'' independent of strain). For Dynamic mechanical analysis (DMA), thicker films (500 μm) were coated on a siliconized PET film and cured in the oven. DMA was performed using a mechanical spectrometer AR 2000 rheometer (TA Instruments) in parallel plate geometry (8 mm diameter and 0.5 mm gap) in dynamic mode with a strain of 0.01. Frequency dependencies of the complex shear modulus at a reference temperature (master curve) were determined from frequency sweeps (from 0.01 to 100 Hz) measured with small amplitude, sinusoidal deformation at temperatures ranging from −50 to +100 °C.

Pressure Sensitive Adhesion. The adhesive strength has been investigated with a 180° peel test as follows: 2 cm wide, 10 cm long stripes were cut and placed on a table (adhesive face on top). Half of the tape length is covered with a second 50 μm-thick PET film, and this assembly is turned upside down. The adhesive area is then applied on the reference surface, and a 2 kg cylinder is rolled twice on the tape. Peel tests were conducted on a Zwick Z005 testing machine at a constant peeling speed of 300 mm/min. The initial adhesion was defined as the peel force measured after a dwell time of 15 min.

RESULTS AND DISCUSSION

Synthesis of Renewable Fatty Polyesters with and without Isosorbide. Polyesters with varying molecular weight and branching degrees have been prepared via bulk polycondensation of dimer fatty acids in combination with one of the three following diols: dimer fatty diol, butane diol, or IS (Figure 1). Because the reaction is a step-growth polymerization, a statistical distribution of chain lengths is obtained, with average molecular weight and chain end-groups controlled by monomer stoichiometry. As we targeted carboxyl-functional polymers, a well-defined excess of diacid was introduced in the reaction vessel and control over polymers molecular weights has been achieved by tuning the monomers stoichiometry.

The extent of polymerization and conversion of acid groups were monitored via GPC and end-groups titration (Table 1). For polyester prepared from aliphatic diols (Pripol 2033 and BDO), the OH values are always negligible confirming that the polymerization proceeds to a point at which the alcohol groups are completely used up and all the chain ends possess the same functional carboxylic acid group in excess. On the other hand, the two IS-containing polyesters both possess a non-negligible residual OH value even after extended polymerization times at 250 °C. Koning et al. made similar observations for a series of acid-terminated poly(IS succinates) and attributed the residual OH values of the polyesters to the difference in reactivity between the two hydroxyl functionalities of IS, the *endo* OH

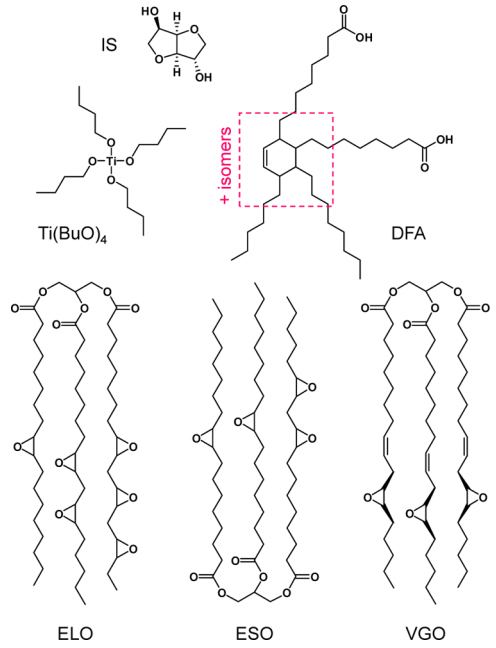

Figure 1. Molecular structures of isosorbide (IS); the dimerized fatty acid (DFA) Pripol 1009; the esterification and transesterification catalyst titanium tetrabutoxide ($Ti(BuO)_4$); and the three epoxy oils mentioned in this study: epoxidized linseed oil (ELO), epoxidized soybean oil (ESO), and *Vernonia galamensis* oil (VGO).

being significantly less reactive than its *exo* counterpart because of intramolecular hydrogen bonding.[24] For linear polyesters (polymers P1 to P6), molecular weight increases as the ratio of diacid to diol monomers nears the stoichiometric equivalence. Polymers P2, P3, and P4 were prepared with an almost equal stoichiometric imbalance of diacid to diol, but the addition of an increasing amount of trimer fatty acid leads to polymers with increasing branching degrees. Increasing the concentration of branching agent is associated with an increase in M_w and a small widening of the polydispersity index, in accordance with Carothers theory of polycondensation.[25]

In practice, the T_g of polymers intended to be used in PSA applications at room temperature generally falls between −15 and −55 °C. As a comparison, polymers P1, P6 and Pi1 had T_g values of −46.3, −46.6, and −17.7 °C, respectively (Table 1), and thus can be considered as potential precursors for PSA. The T_g value of Pi1 also highlights the strong T_g enhancing effect of IS in our system. Overlaid FT-IR spectra of the polymers Pi2 and Pi2 are displayed on Figure 2 (spectrum ii and iii), where the carbonyl groups corresponding to the ester linkages (−COO−) and to the carboxylic acid end groups (−COOH) are clearly visible at 1745 and 1710 cm^{-1}, respectively. The intensity of this later peak is qualitatively related to the acid value of the polyester (and therefore to its molecular weight), although no quantitative estimations could be drawn between these two values. The NMR spectra of polymers P2 and Pi2 are reported in Figure S1 of the Supporting Information and confirm the polymer structures, giving an account of all groups contained in the repeating units, with signals exhibiting the expected area and multiplicity whereas no trace of any other signal could be detected in the spectra.

Choice and Properties of the Bio-Derived Epoxy Cross-linkers. This work reports the design of fully renewable adhesive compositions obtained by cross-linking acid-functional

dx.doi.org/10.1021/ma400203v | Macromolecules 2013, 46, 3395−3405

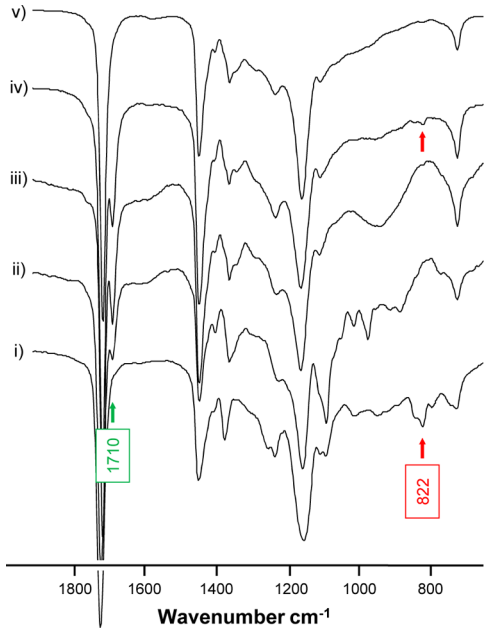

Figure 2. Overlaid FTIR spectra of the cross-linker ELO (i), polymers Pi2 (ii) and P2 (iii), the adhesive formulation P2−10%ELO in the uncured state (iv), and after curing at 155 °C for 15 min (v). The peaks at 1710 and 822 cm^{-1} correspond to the carbonyl group of the carboxylic acid (−COOH) and to the oxirane ring, respectively.

polyesters with epoxidized triglycerides (ELO, ESO and VGO). Up to now, epoxidized natural oils have mainly been used as plasticizers for PVC and as precursors for highly cross-linked thermosets.[26−28] In addition, Overeem et al. applied epoxidized oils showing high percentages of oxirane oxygen (ELO and the naturally epoxidized *Lallemantia iberica* oil) as renewable cross-linkers in powder coating formulations.[29,30] However, a potential problem associated with aliphatic fatty oxiranes in powder-coatings is the plasticizing effect of the fatty acid backbone that tend to decrease the T_g of the resulting resins. As a result, toxic epoxy compounds such as triglycidyl isocyanurate (TGIC) are still employed in powder coating resins, even when the biobased polymers of these resins are fully derived from renewable resources.[24,31] In contrary, the low glass temperature transition of natural oils can turned out to be an advantage for the design of PSA, where a low T_g is a prerequisite.

Two commercially available epoxidized plant oils with different oxirane functionality, namely epoxidized linseed oil (ELO) and epoxidized soybean oil (ESO) were considered in this study. In addition, *V. galamensis* oil (VGO), which is obtained from the seeds of *V. galamensis* (a shrub of the Compositae family native to northern and central Africa)[32] has also been tested here as a naturally occurring biocrosslinker. This oil is composed of triacylglycerols containing about 75% of *cis*-12,13-epoxy-*cis*-9-octadecenoic acid, a naturally epoxidized fatty acid known as vernolic acid, and possess a lower epoxy functionality as compared to ELO and ESO (Table 2).[33] The FT-IR of ELO reveals the ester band of the triacylglycerol at 1745 cm^{-1}, in addition to the epoxy-related peak at 822 cm^{-1} in Figure 2 (spectrum i). The three epoxy compounds were further characterized by titration, as shown in Table 2. Although the acid values of ELO and ESO are both negligible, VGO has an acid value of 1.09 mg of KOH/g, revealing a tiny fraction of free fatty acid.

Table 2. Properties of the Epoxy Bio-Oils

item	AV (mg KOH/g)	epoxy value (mg KOH/g)	M_w (g/mol)
ELO	0.24	299.63	1587
ESO	0.25	232.69	1541
VGO	1.09	147.28	1452

Percolative Step-Growth Reaction Between Carboxylic-Acid-Terminated Polyesters and Epoxidized Plant Oils. Three reactions have to be envisaged during the cure of epoxides with carboxylic acids (Figure 3): the addition-esterification reaction between a carboxylic acid and an oxirane giving rise to a β-hydroxyester (path A), the etherification of an epoxide with an alcohols (path B), and the condensation−esterification of a carboxylic acid by an alcohol (path C). FT-IR spectra of the adhesive P2−10%ELO before and after 15 min curing at 155 °C is shown in spectra iv and v of Figure 2, respectively. Because of the low concentration of epoxy groups in the system, the oxirane adsorption band at 822 cm^{-1} is barely visible even in the uncured state and could not be use to quantitatively assess the degree of curing of the system. A more convincing spectroscopic evidence of the curing reaction is obtained by following the sharp decrease of the carboxylic acid band at 1710 cm^{-1} (consumption of the polyester end-group), and the concomitant increase of the ester band at 1745 cm^{-1}, which is consistent with the curing path A of Figure 3.

Figure S2 of the Supporting Information depicts the evolution of the storage modulus G' and loss modulus G'' during isothermal cure at 155 °C for the adhesives P1−8.75% ELO and P1−25%ELO. At the beginning the real part of the shear modulus G' was lower than the imaginary part (the loss modulus G'') denoting a liquid-like response. Upon curing, both G' and G'' increased, but the build-up rate of G' is higher than that of G'', and a crossover occurred after 6 min for P1−25%ELO. This crossover defines an easily accessible characteristic time for all reactive systems. After this point, G' kept increasing, whereas G'' tend to reach a plateau corresponding to a more solid-like behavior with a high elastic part (G') compared to the viscous contribution (G''). Figure 4A displays the evolution of the loss factor $\tan(\delta)$ as a function of time during the isothermal cure of P1−8.75%ELO at different temperatures.

According to Flory's gelation theory,[34] the chemical conversion of a thermosetting resin at the gel point is constant and not related to the reaction temperature and/or to the experimental conditions. As a result, the apparent activation energy ΔE_a of the cure reaction can be estimated from the crossover time between the $[\tan(\delta) = f(t)]$ and $[\tan(\delta) = 1]$ curves according to eq 1, where C is a constant, R is the gas constant, and T is the cure temperature:

$$\ln(t_{GEL}) = C + \left(\frac{\Delta Ea}{RT}\right) \quad (1)$$

Figure 4B shows a plot of $\ln(t_{GEL})$ as a function of the reciprocal temperature for the system P1−8.75%ELO and five other adhesives prepared from different combinations of base-polymers and cross-linkers. For each formulation, the good parallel fits indicate that the observed cure reaction is in good agreement with eq 1, and that the activation energy of the cure reaction does not depend on the base polymer employed nor on the type and functionality of the cross-linker (ELO, ESO, or VGO). It is also noteworthy that the activation energy of the cure reaction seems rather similar for adhesives prepared from polyesters with or without IS (Figure 4B, specimen Pi2−20%

dx.doi.org/10.1021/ma400203v | *Macromolecules* 2013, 46, 3395−3405

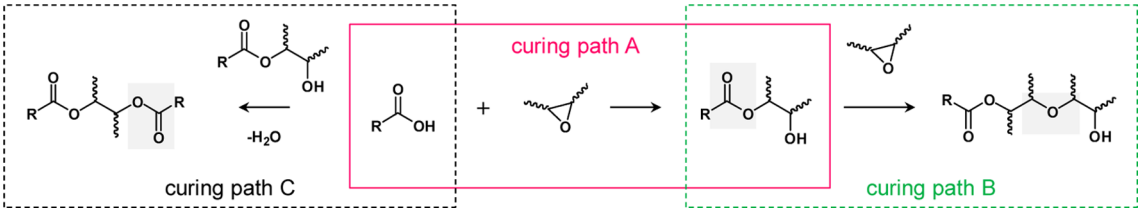

Figure 3. Scheme of the possible curing pathways: addition esterification of the polyester carboxylic acids end-groups with the multifunctional epoxy cross-linker (path A), ether formation between oxirane and hydroxyl groups (path B), and condensation esterification between carboxylic acid and hydroxyl functionalities (path C).

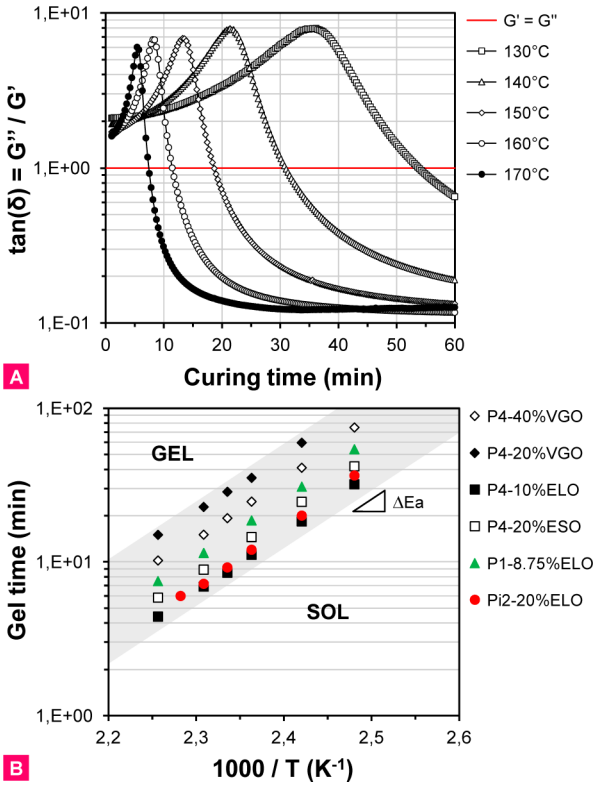

Figure 4. (A) Loss factor tan(δ) versus reaction time for the adhesive P1−8.75%ELO cured at different temperatures; (B) Arhenius plot of the gelation time (as defined by the crossover between G' and G'') as a function of the reciprocal temperature for six adhesives obtained from various combination of network precursors.

ELO). This might be an indication that the remaining hydroxyl groups that are always present in the IS-based polymers are not participating to the cure reaction, and that the catalytic conditions promote the addition-esterification while minimizing the two competitive side reactions involving hydroxyl groups. According to Blank et al.,[35] the efficient catalytic mechanism of Nacure XC-9206, a zinc chelate (ZnCH) compound, on the epoxy-acid reaction is attributed to the property of Zinc to function as a base at high temperatures and to form a carboxyl anion leading to an attack of the epoxy group (see details on Figure S3 of the Supporting Information).

Development and Fractal Dimension of the Gelified Architectures. A gelling system at the critical gel point becomes viscoelastic [tan(δ) ~ 1] due to the infinite tree-like self-similar fractal structure comprising many branched chains.[36,37] The Creton group recently demonstrated that the structure of this percolated cluster combined with a high sol fraction is essential in PSA systems, notably for increasing the cohesive strength of the adhesive while maintaining good tack values.[38−40] In order to better characterize and understand the adhesive properties of our renewable PSA, it is informative to investigate in more details the fractal structures of our adhesives near the gel point, and this can be achieved by having a closer look at the sol−gel transition. As an alternative to eq 1, Winter and Chambon proposed to define the gel point by the instant at which both G' and G'' follow a scaling law of the form $G' \approx G'' \approx \omega^n$, where n is a relaxation exponent intimately correlated to the structure of the gel.[41] The factor n is independent of the frequency but proportional to tan(δ) as expressed by $\tan(\delta) = \tan(n\pi/2) = (G''/G')$. As a result, n can be determined by performing isothermal cure kinetics and by playing with the frequency of the dynamic mechanical stimulation as the only experimental parameter, as shown on Figure S4 of the Supporting Information for the system P1−10%ELO cured at 155 °C. The relaxation exponent n can be further correlated to the fractal dimension (D_f) of the gel according to eq 2 (in the case of a three-dimensional space).

$$n = \frac{3(5 - 2D_f)}{2(5 - D_f)} \tag{2}$$

The fractal dimension gives insight into the complexity of the a system at the gel point, and notably on how compact or open is the macromolecular architecture. In general, one observes $D_f \leq 3$, with $D_f < 3$ indicating an open structure and $D_f = 3$ a dense structure. We obtained $n = 0.42$ ($\pm 3.1 \times 10^{-2}$) and $D_f = 2.10$ ($\pm 3.5 \times 10^{-2}$) for the system P1−10%ELO, which is characteristic of a relatively open structure such as those observed in loosely cross-linked materials like PSAs and elastomers.

A schematic representation of the branching points constituting the tree-like architecture of our adhesive is displayed on Figure 5 and illustrates that all the structural elements of the networks are fully based upon ester linkages (assuming that the addition condensation is the major curing mechanism).

Correlation Between Stoichiometry, Gel Content, and Shear Elastic Modulus. The structure of networks formed by step-growth polymerization of polyfunctional precursors is largely influenced by the functionality of the monomers and the extent of the cure reaction. While highly functional precursors will lead to densely cross-linked systems with high elastic modulus, low functionality tend to produce softer networks with defects such as free molecules (sol), dangling chains or loops.[42] These substructures are not elastically active and do not contribute to the elastic modulus, but they are responsible for the longer relaxation times and damping properties that are so important in PSA.

Figure 6A illustrates how the gel content of various cured adhesives correlates with the compounding ratio of epoxy

dx.doi.org/10.1021/ma400203v | Macromolecules 2013, 46, 3395−3405

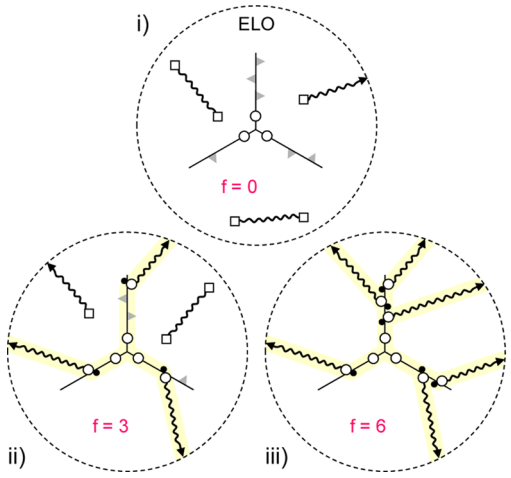

Figure 5. Schemes of an unreacted mixture of ELO and a COOH-terminated polymer (i), and hypothetical structures of two percolation sites with functionalities of three (ii) or six (iii): (●) −OH; (○) −COO−; (□) −COOH; (▲) epoxy. Black arrowheads (⇝) indicate continuation of the network structure.

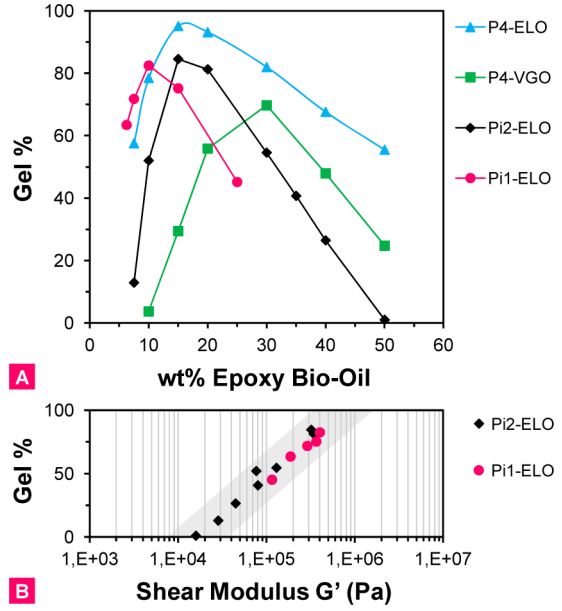

Figure 6. (A) Gel content versus epoxy concentration for the networks P4-β%ELO P4-β%VGO, Pi1-β%ELO and Pi2-β%ELO; (B) Correlation between gel % and shear modulus for Pi1-β%ELO and Pi2-β%ELO gels.

cross-linker. For every P$\alpha-\beta$%γ system, there exists a specific stoichiometry corresponding to an optimal gel fraction and elastic modulus (see also Figure S5 of the Supporting Information). According to eq 3 (where Θ is the conversion at the gel point, r is the molar ratio of the two different types of functional groups (with $1 \geq r$), and f and g are, respectively, the average functionalities of the acid and epoxy compounds), the precursors ratio corresponding to optimal physical properties should correspond to a stoichiometric balance of epoxy and carboxylic acid groups in the reactive formulation.[43]

$$\Theta = \sqrt{\frac{1}{r(f-1)(g-1)}} \qquad (3)$$

However, this was never observed experimentally and an excess of epoxy was systematically needed to achieve the highest gel fractions for a given system. This stoichiometric excess of epoxy functionalities is different for each formulation and typically vary from 1.8 for the gel P4-β%ELO to 1,4 for the system P4-β%VGO.

Different reasons can be evoked to explain the discrepancy between the experimental and theoretical optimal stoichiometries. At first, poor accessibility of cross-linking sites due to restricted diffusion of reactive groups during gelation could be anticipated.[44,45] This limited diffusion could also be reinforced by the steric hindrances associated with the bulky character of our fatty-acid-based polymers and cross-linkers. For instance, Zhang et al. recently noted that during the ring-opening polymerization of ELO, when one epoxy group reacts, the other group adjacent to it has a very low reactivity as a result of the large steric hindrance.[26] Second, the need for an excess of epoxy compound could also be attributed to a nonideal cross-linking behavior.[46,47] Such a nonideal curing process would not be really surprising considering that besides the fluctuations in network density caused by the statistical cross-linking process, the adhesive precursors such as natural triglycerides are nonideal molecules themselves. Nevertheless, this macromolecular diversity can turn out to be useful for designing PSA as it is expected to produce softer critical gels and will bring to the material a number of relaxation modes with widely different characteristic times and strengths that are necessary for obtaining good PSA.[42]

Control over the sol/gel content is a key parameter for the design of functional PSA and is related to the ability of the material to dissipate energy through deformation. It is evident from Figure 6A that the gel content can be easily and reproducibly manipulated by tuning the formulation ratio and can be adjusted anywhere from 20 to 90%. As a matter of comparison commercial PSAs typically contain about 50−70% of insoluble fraction, which is in good agreement with some of the values reported on Figure 6A As expected from eq 3, a given polymer (for instance P4) formulated with a highly functional cross-linker like ELO display higher gel contents than the same polymer cured with a low functionality epoxydised triglycerides such as VGO. In addition, the gel contents of the adhesives correlate well with their elastic modulus G', confirming that both parameters are related to the concentration of elastically active chains within the networks (Figure 6B).

Probing the Viscoelastic Nature of the Renewable Sticky Resins. The mechanical analysis of the biobased adhesives has been characterized by the frequency dependencies of G' and G'' determined in dynamic deformation experiments with sinusoidal signals in the linear viscoelastic regime. The reported dependencies on Figures 7 and 8 are master curves obtained by frequency shifts of raw data obtained at various temperatures and referenced at 25 °C as a function of the reduced frequency ($\omega.a_T$). Time−temperature superposition (TTS) was satisfied in all cases, revealing that all the relaxation processes have similar temperature dependencies.[48]

Figure 7A shows a representative viscoelastic spectrum obtained for the adhesive Pi1−6.25%ELO, and indicates two main relaxation modes detected at high and low frequencies, respectively. The fastest process corresponds to the segmental relaxation ($\tau_{seg.}$) of polymeric units and is therefore a short-range phenomena involving only few monomers.[49,50] The slower mode is a much broader process and can be attributed to

dx.doi.org/10.1021/ma400203v | Macromolecules 2013, 46, 3395−3405

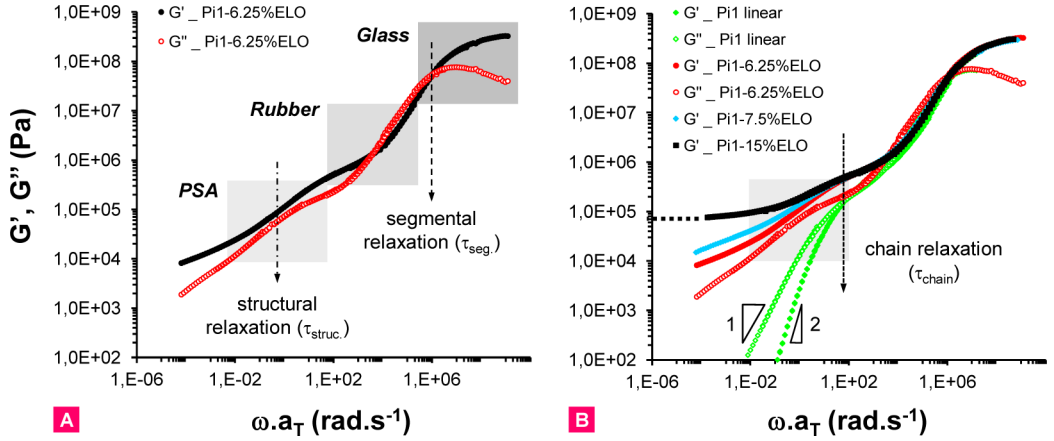

Figure 7. (A) Reduced frequency ($\omega.a_T$) dependency of the real (G') and imaginary (G'') shear modulus components for the adhesive Pi1−6.25% ELO. (B) Effect of the cross-linking density on the viscoelastic spectrum of Pi1-β%ELO gels.

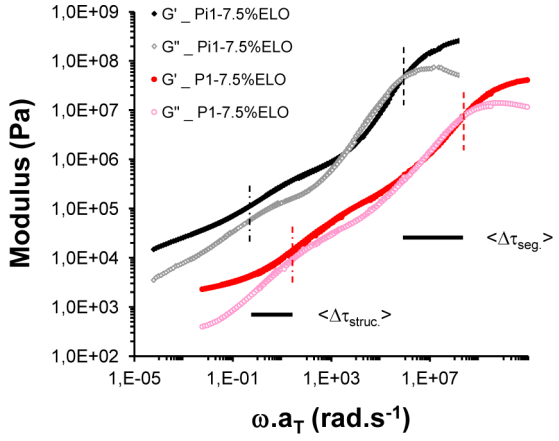

Figure 8. Real (G') and imaginary (G'') shear modulus components for the adhesives Pi1−7.5%ELO (IS-based) and P1−7.5%ELO (purely fatty acid-based) plotted against the reduced frequency.

the combined structural relaxations ($\tau_{struc.}$) of the gel architecture (the fractal tree-like structure) and of the network defects (dangling chains and sol fraction). Because the system Pi1−6.25%ELO is partially cross-linked, the mobility of polymer chains is not sufficient for a global (flow) relaxation to occur (thus $G' > G''$ over the whole frequency range). On the other hand, the cross-linking density of this sample is still rather low and no characteristic rubbery plateau could be clearly detected at low frequencies, at least in the temperature range investigated.

Depending on the frequency of the mechanical solicitation, Pi1−6.25%ELO can behave either as a glass, a rubber, or a viscoelastic material with PSA-like properties. The practical PSA range has been schematically represented on Figure 7A by a light-gray window where the two vertical lines defining the square at 10^{-2} rad.s^{-1} and 10^{2} rad.s^{-1} correspond approximately to the rate of bond establishment of a tape and to the debonding of an adhesive layer, respectively. It is generally accepted that good PSA should exhibit a dynamic shear modulus $G' < 1 \times 10^5$ Pa at 1 Hz or alternatively a tensile (Young's) modulus $E < 3 \times 10^5$ Pa (as $E = 3 \times G$ for incompressible materials) in order to promote wetting and maximize contact with the adherent.[51,52] The shear modulus of Pi1−6.25%ELO ($G' = 1.8 \times 10^5$ Pa) is slightly above the Dahlquist criterion, but still acceptable for a PSA since both the M_w of the precursors and the cross-linking density are low.

Figure 7B demonstrates how the cross-linking density of the biobased adhesives induces profound modifications on their viscoelastic spectrum. For linear polymers such as Pi1, the structural relaxation does not occur and is replaced by a chain relaxation (τ_{chain}) associated with global flow ($G'' > G'$) and chain disentanglement at intermediate frequency. In this case, the characteristic slopes of viscoelastic fluids ($G' \sim \omega^2$ and $G'' \sim \omega$) are observed at low frequencies in accordance with the Maxwell model of relaxed chains. In the high frequency region ($\omega > 10^5$ rad·s^{-1}), the viscoelastic spectrum of all Pi1-β%ELO gels tend to superimpose irrelevantly of ELO amount (Figure 7B), because stress relaxation in this domain is controlled by short-range motions involving only few monomer units and does not depend on topological factors. The high frequency superposition of the viscoelastic spectrum indicates that the T_g of Pi1-β%ELO gels is not influenced by the network cross-linking density.

A limited amount of cross-linking is sufficient to suppress the global flow of free chains and introduce the structural relaxation mode ($\tau_{struc.}$) characteristic of percolated structures. The fact that this structural relaxation is always shifted to lower frequencies as compared to the linear chain relaxation confirms that extensive chain-extending and branching occurred during the curing process, because molecular conformations relax with slower modes as the macromolecular size increases. The height and amplitude of the low-frequency rubbery plateau develops itself progressively with the increasing cross-linking density, and ultimately Pi1−15%ELO present a viscoelastic spectrum resembling the one of an elastomer.[53]

Comparative Rheological Spectra With and Without IS. Figure 8 shows the viscoelastic spectra obtained for the two systems Pi1−7.5%ELO and P1−7.5%ELO, both having a rather similar gel content around 70% but respectively designed with and without IS. A complete shift of the rheological curves toward lower frequencies is observed for the IS-based polymers, involving both the segmental ($\Delta\tau_{seg.}$) and structural ($\Delta\tau_{struc.}$) relaxations. These frequency shifts reveal the higher T_g of Pi1−7.5%ELO and the increased stiffness of polymer chains containing bicyclic *cis*-fused tetrahydrofuran rings. As a consequence, the elastic modulus of Pi1−7.5%ELO within the PSA frequency-window is five times higher than the modulus of P1−7.5%ELO, meaning that despite these two

dx.doi.org/10.1021/ma400203v | *Macromolecules* 2013, 46, 3395−3405

adhesives possessing quite similar cross-linking densities, the IS-containing network is more cohesive than its purely fatty-acid counterpart. A small vertical shift ($\Delta G'$) is also observed between these two loosely cross-linked gels indicating that even in the glassy state, the adhesive without IS remains softer than Pi1−7.5%ELO. In the case of more cross-linked rubber-like samples such as Pi1−15%ELO and Pi1−15%ELO, the frequency shifts ($\Delta\tau_{seg.}$ and $\Delta\tau_{struc.}$) are still clearly observed, but the vertical shift of G' is greatly reduced (Figure S7 of the Supporting Information).

Tape Construction and Adhesion Testing. Adhesive formulations containing the base polymer, the epoxy cross-linker, and the Nacure catalyst were diluted with toluene to obtain a global solid base of 70%, and this solution was roll-coated onto a base film before being thermally cured at 155 °C. After curing of the glue layer, the resulting tapes displayed interesting self-adhesives properties as exemplified on Figure 9A. As the peel force a tape is not only determined by the properties of the glue layer itself but is also strongly influenced by the adhesive layer thickness and the flexural rigidity of the backing film, all adhesion measurements were performed with 20 μm-thick layer of glues (dry thickness) coated on the same 50 μm-thick PET film. Three different debonding modes were observed throughout the course of our investigations, namely interfacial failure (clean removal, see Figure 9C), cohesive failure (this applies when residual sticky patches are left on the substrate after peel, or when the adhesive layer is completely splitted in two parts following the break of large cohesive fibrils, as shown on Figure 9B), and failure at the adhesive-PET film interface.

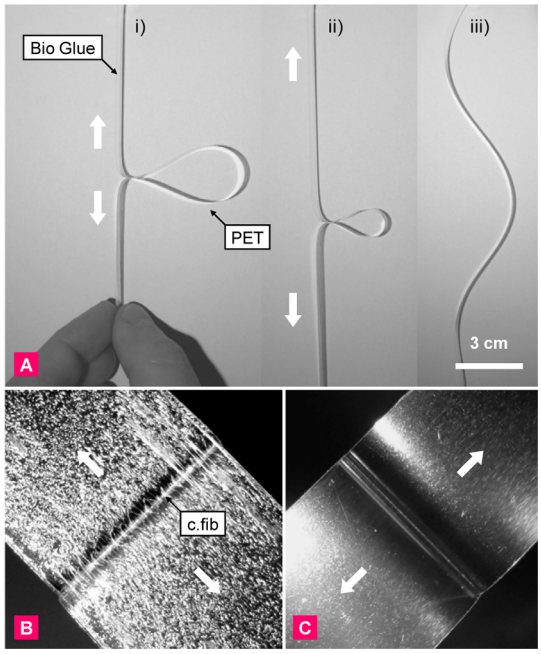

Figure 9. (A) Cross-section images illustrating the self-adhesive properties of a biobased tape (IS-based glue Pi1−7.5%ELO coated on PET) forming an internal loop (i). The loop shrinks progressively upon tearing of the tape (ii) before being ultimately released (iii); (B, C) Front-view of the peeling zones for the systems Pi2−7.5%ELO (B, cohesive failure) and Pi1−7.5%ELO (C, interfacial failure). Width of the tapes was 2 cm in each case. White arrows indicate direction of the peel force. c.fib: cohesive fibrils.

Bulk Factors Impacting Adhesion at the Macroscopic Level. The correlation between the bulk viscoelastic properties of PSAs at small strain and their adhesion performance is well-established.[5,6] Bonding is a low frequency process and is the result of the adhesive being able to flow and wet the substrate under light pressure. On the other end, the debonding step can be regarded as a high rate phenomenon involving the deformation of the adhesive layer under stress. In practice, the optimal balance between cohesion and adhesion can be elusive to determine and strongly depends on the base polymer characteristic and cross-linking density.

Figure 10 displays the initial adhesion forces of Pi2-β%ELO, Pi1-β %ELO, and P3-β %ELO adhesives as a function of the network formulation from PC and steel substrates. As expected, adhesion levels and debonding modes are strongly influenced by the compounding ratio of the adhesives. When a given tape fails cohesively on both PC and steel, the measured peel forces mostly correspond to the cohesive strength of the glue and are not influenced by the substrate type. In case of an interfacial debonding, the IS-based adhesives adhere more strongly on PC than on Steel, whether IS-free adhesives (P3-β%ELO) show an opposite trend. As previously demonstrated, the compounding ratio of the adhesives influence both the gel content (Figure 6) and rheology (Figure 7) of the networks. In order to fully elucidate the adhesion trends observed on Figure 10, it is interesting to investigate how the adhesion profiles of the gels could be related to their gel contents. To this end, Figure 11 summarizes the relation observed between initial adhesion, gel content, debonding mode and rheology for the IS-based adhesives Pi1-β%ELO and Pi2-β %ELO.

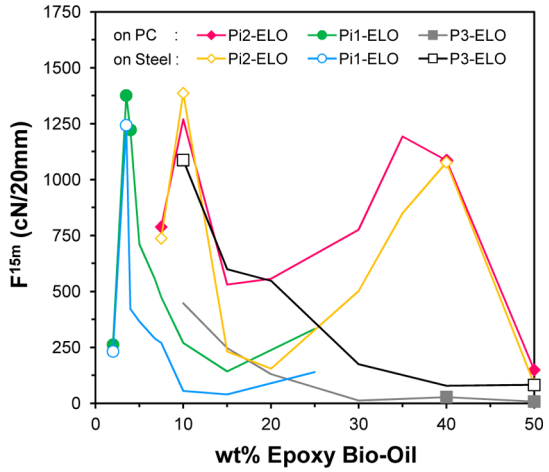

Figure 10. Initial peel forces (F^{15m}) for the systems Pi2-β%ELO, Pi1-β%ELO, and P3-β%ELO on polycarbonates (PC) and steel substrates. The absence of symbols on the lines corresponds to an interfacial failure (clean removal), whether the symbols indicate cohesive failures.

Considering first Pi2-β%ELO glues, it appears from Figure 11B that samples with the highest gel fractions (Pi2−15%ELO and Pi2−20%ELO) display the lowest adhesion levels because their adhesion hysteresis are not large enough to cause the formation of fibrils and lead to a quick crack propagation. Deviations from this optimal cross-linking ratio (from both sides of the stoichiometric equivalence) gradually produce adhesives with lower gel fraction and higher dissipative character resulting in increased adhesion (Pi2−30%ELO). Ultimately, high adhesion forces (above 1000 cN/20 mm)

dx.doi.org/10.1021/ma400203v | Macromolecules 2013, 46, 3395−3405

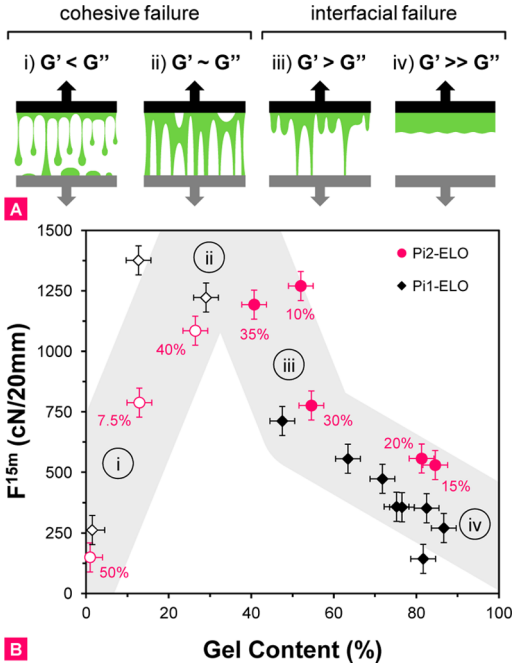

Figure 11. (A) Schemes of the debonding patterns observed for Pi2-*β*%ELO adhesives in relation with their rheological profiles. The upper (black) plate corresponds to the PET film. Key: (i) viscous fibrils; (ii) cohesive fibrils; (iii) interfacial fibrils; (iv) crack propagation. (B) Initial peel force (F^{15m}) versus gel content for Pi2-*β*%ELO and Pi1-*β*%ELO tapes peeled from PC. Filled and empty symbols corresponds to interfacial and cohesive failure modes, respectively. The gray zone is a guide for the eye.

are obtained for the two networks Pi2−10%ELO and Pi2−35%ELO displaying gel contents of 52% and 41%, respectively. These adhesives display an optimal balance between cohesive and dissipative characters and exhibit interfacial fibrils upon debonding.

Further stoichiometric deviations induce a transition from interfacial to cohesive failure associated with considerable legging requiring a large deformation to cause debonding (Pi2−40%ELO), and ultimately a transition from rubber-like elastic to liquid-like viscous behavior (Pi2−7.5%ELO, Pi2−50%ELO). In this later cases, the networks do not possess the necessary mechanical strength and too much adhesive bonding comes at the expense of cohesion. The failure modes of Pi2-*β*%ELO adhesives schematically represented on Figure 11A correlates well with their respective viscoelastic profiles, as exemplified by the Cole−Cole diagram of Pi2-*β*%ELO networks displayed on Figure S8 of the Supporting Information. Similar observations can be made for the system Pi1-*β*%ELO, although in general these adhesives tend to display lower initial adhesion levels than Pi1-*β*%ELO for a given gel content (Figure 11B). As Pi1-*β*%ELO has been formulated with a polymer of higher M_w, the reduced diffusion of polymer chains could result in a slower wetting and lower initial affinity for the surface.

In summary, formulation of the lipid-based adhesives can be used to adjust the gel content of the glues, which in turns provide an efficient way to fine-tune the cohesive strength of the gels and adjust the peel force by controlling the extent of fibril formation. Although this article only reports the adhesion properties of coatings cured with ELO, it is notable that interesting results were also obtained with adhesives cured with ESO or even VGO. However, VGO-based adhesives tend to display lower gel content and consequently often fails cohesively. It should also be noted that the reported adhesion data are always determined from neat (unformulated) polymeric samples. This simplification allows us to better isolate the effect of IS in the system. However peel, tack, and cohesion properties may be improved though the incorporation of (renewable) additives and tackifiers that will further adjust the glass transition temperature and lower the modulus by diluting topological entanglements.

Nanoscale Parameters Influencing Adhesion at the Molecular Level. Upon aging on a substrate, it is known that most PSA experienced complicated surface restructuring processes that influence the strength of the adhesive bond.[54] Ultimately, the global strength of the joint stems from by a delicate balance between the viscoelastic character of the glue and the increased interfacial structure resulting from macromolecular rearrangements and the development of a 2D network of noncovalent interactions near the adhesive/substrate interface.[55] Here, a basic aging has been performed in order to investigate the potential surface restructuring effects of polyester adhesives formulated with or without IS. Figure 12

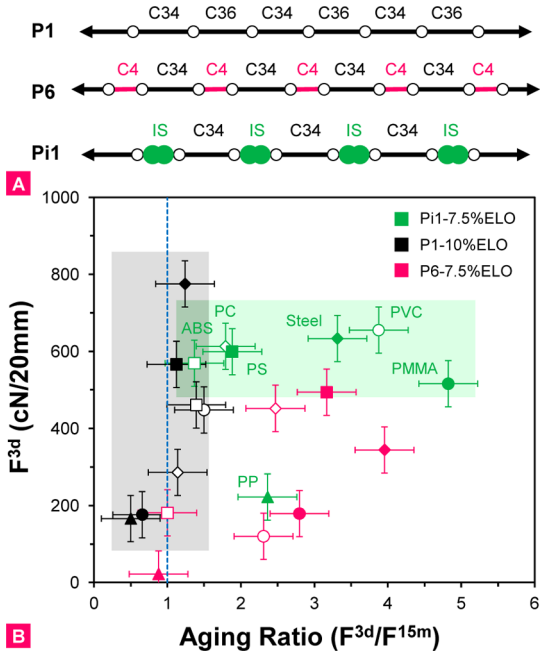

Figure 12. (A) Alternating structures of P1, P6 and Pi1; B) Adhesion after 3 days of aging (F^{3d}) versus the aging ratio (F^{3d}/F^{15m}) for P1−10%ELO, P6−7.5%ELO and Pi1−7.5%ELO on various substrates: steel (♦); PC, polycarbonate (◊); PMMA, poly(methyl methacrylate) (●); PVC, polyvinyl chloride (○); PS, polystyrene (■); ABS, acrylonitrile butadiene styrene (□); PP, polypropylene (▲). All tapes failed in an interfacial manner. The dotted line refers to even adhesion forces before and after aging.

reports the adhesion forces measured after a three-days dwell time at room temperature as a function of the aging ratio (aged adhesion/initial adhesion) for the adhesives P1−10%ELO, P6−7.5%ELO, and Pi1−7.5%ELO on various substrates.

For purely fatty-acid-based adhesives such as P1−10%ELO, a very low increase of adhesion is consistently observed after three days (Figure 12B) suggesting that only a very limited restructuration occurred. The lack of adhesion enhancement of P1−10%ELO upon aging can be attributed to the low polarity of this adhesive. Indeed, the carboxylic acid end-groups of the

dx.doi.org/10.1021/ma400203v | *Macromolecules* 2013, 46, 3395−3405

base polymer have been consumed during the curing process and the only polar elements of the glue are the ester groups of the base polymers, the β-hydroxy ester linkages at the branching sites, and eventually some residual epoxy groups. In addition, the adhesion level of P1−10%ELO after aging strongly depends on the type of substrate.

In contrast to the above-mentioned observations, major adhesion enhancements are observed on all substrates for the adhesive Pi1−7.5%ELO. After three days, an almost equal level of adhesion is obtained on all substrates (see also the corresponding peel curves on Figure S9 of the Supporting Information), except on PP which has the lowest surface tension of all substrates. This pronounced surface restructuring can be reasonably attributed to the higher polarity of Pi1−7.5% ELO, stemming from the increased concentration of ester bonds in Pi1 as compared to P1 and from the presence of the sugar-based IS moieties. As a comparison, the adhesive P6−7,5%ELO also demonstrate some adhesion enhancement upon aging, but to a lower extent than Pi1−7.5%ELO (ester concentration in P6 is even higher than in Pi1, but P6 does not contain IS, as schematically represented on Figure 12A). This comparative example suggests that ester linkages are not solely responsible for the surface restructuring observed with Pi1−7.5%ELO, but that the IS groups are effective for restructuring the near-surface topology of the adhesives and establishing various non covalent interactions with the different adherents.

Overall, we have presented here model IS-based tapes and compared the adhesion results with adhesives formulated without IS. Despite the obvious differences observed in terms of T_g, rheology and adhesion profiles, it is very difficult at this stage to definitely elucidate the role of IS in pressure sensitive adhesion. PSAs are extremely complex and multiform materials that should simultaneously possess ambivalent properties such as high molecular mobility, long relaxation times, substantial cohesive strength and conformational restructuration upon aging.[56] As we have exemplified in this paper, IS impacts all these interrelated parameters in a nontrivial manner, and additional experiments will be necessary to separate the bulk and the interfacial effects of IS on adhesion. This may be achieved by fabricating multilayer adhesives,[57] where IS groups are only present near the adhesive/adherent interface and not in the bulk of the glue layer or vice versa.

CONCLUSION

Recent advances in PSA have witnessed the emergence of polyesters[9,10,58−60] as a credible alternative to the standard chemistries. The interest in polyester chemistry is triggered by its intrinsic sustainable advantages: polyesters are readily synthesized in bulk, they tend to degrade in an environment-friendly manner,[61,62] and a wide range of polyester building blocks are gradually becoming available from biorefineries.[4,11,12] Fundamentally, this article exemplifies that some well-established design principles of petrochemical-based adhesives (such as adjusting the cohesion of PSA by adding a small fraction of high-T_g monomer into low-T_g monomers)[5] could be advantageously transposed to the world of green chemistry in view of speeding-up the emergence of functional biobased PSA solutions. The use of IS as a building block for soft materials is also rather unique and open interesting perspectives in polymer science, notably toward the life-sciences where tunable stickiness, functionality, nontoxicity and potential degradability are important requirements for innovative biomaterials. The "art" of formulating and optimizing the performances of self-adhesive polyester materials is only emerging and yet to be fully mastered, in view of developing eco-friendly adhesive solutions that stick to the society's sustainable needs.

ASSOCIATED CONTENT

Supporting Information

Remarks on the peel tests, NMR spectra of polymers P1 and Pi1; evolution of G' and G'' with the curing reaction time, detailed catalytic mechanism of the curing reaction, and additional rheology and adhesion data. This material is available free of charge via the Internet at http://pubs.acs.org.

AUTHOR INFORMATION

Corresponding Author

*(R.V.) E-mail: richard_vendamme@nittoeur.com, Tel: + 32-(0)89-36 04 95. Fax +32-(0)89-36 22 42.

Notes

The authors declare the following competing financial interest(s): Nitto Europe N.V. (Belgium) and Nitto Denko Corp. (Japan) co-owned the patent applications WO/2011/023255, EP2290000, US/2012/0156484, WO/2012/072237 and EP2460864 disclosing biobased adhesive compositions crosslinked with functionalized triglycerides and the patents applications WO/2012/045480 and EP2439224 that teach adhesives and compositions containing a heterobicyclic compound such as isosorbide.

ACKNOWLEDGMENTS

The authors are grateful to the top management of Nitto Denko for allowing the publication of this work and especially to Toshihiko Omote for his support and confidence. Partial financial support from the Institute for the Promotion of Innovation through Science and Technology in Flanders (IWT-Vlaanderen) is duly acknowledged. We would like to thank Frank Thumerel and Hervé Wyart (Roquette Frères) for providing the high purity IS, Ingrid Wasbauer (Nitto Europe N.V.) for the GPC measurements, and Geert Pirrote (Hasselt University) for his contribution to this project as an internship bachelor student. The authors also thank Satoshi Tanigawa, Tetsuo Inoue, Masatsugu Higashi, Hitoshi Takahira, Satomi Yoshie, Shigeki Ishiguro, Takayuki Shigematsu, and Tetsuya Iwai (Nitto Denko Corp.) for insightful discussions on biobased chemistry and adhesion technology.

REFERENCES

(1) *Monomers, Polymers and Composites from Renewable Resources*; Belgacem, M. N., Gandini, A., Eds.; Elsevier: Oxford, U.K., 2008.
(2) Wool, R. P.; Sun, X. S. *Bio-Based Polymers and Composites*; Elsevier: Boston, 2005.
(3) Gandini, A. *Macromolecules* **2008**, *41*, 9491−9504.
(4) Bozell, J.; Petersen, G. R. *Green Chem.* **2010**, *12*, 539−554.
(5) *Handbook of Pressure Sensitive Adhesive Technology*, 2nd ed.; Satas, D., Ed.; Springer: New York; 1989.
(6) Creton, C. *MRS Bull.* **2003**, *28*, 434−439.
(7) Zosel, A. *Adv. Pressure Sensitive Adhes. Technol.* **1992**, *1*, 92−127.
(8) Peykova, Y.; Guriyanova, S.; Lebedava, O.; Diethert, A.; Muller-Bushbaum, P.; Willenbacher, N. *Int. J. Adhes. Adhes.* **2010**, *30*, 245−254.
(9) Ozturk, G I.; Pasquale, A. J.; Long, T. E. *J. Adhes.* **2012**, *86*, 395−408.
(10) Vendamme, R.; Olaerts, K.; Gomes, M.; Degens, M.; Shigematsu, T.; Eevers, W. *Biomacromolecules* **2012**, *13*, 1933−1944.

(11) Biermann, U.; Bornscheuer, U.; Meier, M. A. M.; Metzger, J. O.; Schafer, H. J. *Angew. Chem., Int. Ed.* **2011**, *50*, 3854−3871.
(12) Hill, K. *Pure Appl. Chem.* **2007**, *79*, 1999−2011.
(13) Koch, C. A. Patent WO/2008/144703.
(14) Ahn, B. K.; Fraft, S.; Wang, D.; Sun, X. S. *Biomacromolecules* **2011**, *12*, 1839−1843.
(15) Bunker, S. P.; Staller, C.; Willenbacher, N.; Wool, R. P. *Int. J. Adhes. Adhes.* **2003**, *23*, 29−38.
(16) Wool, R. P.; Bunker, S. P. *J. Adhes.* **2007**, *83*, 907−926.
(17) Serrero, A.; Trombotto, S.; Bayon, Y.; Gravagna, P.; Montanari, S.; David, L. *Biomacromolecules* **2011**, *12*, 1556−1566.
(18) Bloembergen, S.; Mclennan, I. J.; Schmaltz, C. S. *Adhes. Technol.* **1999**, *9*, 10−13.
(19) Bloembergen, S.; Mclennan, I. J.; Cassar, S. E.; Narayan, R. *Adhes. Age* **1998**, *41*, 20.
(20) Stoss, P.; Hemmer, R. *Adv. Carbohydr. Chem. Biochem.* **1991**, *49*, 93−173.
(21) Fenouillot, F.; Rousseau, A.; Colomines, G.; Saint-Loup, R.; Pascault, J. P. *Prog. Polym. Sci.* **2010**, *35*, 578−622.
(22) Kricheldorf, H. R. *J. Macromol. Sci., Rev. Macromol. Chem. Phys.* **1997**, *C37*, 599−631.
(23) Noordover, B. A. J.; Duchateau, R.; van Benthem, R. A. T. M.; Ming, W.; Koning, C. E. *Biomacromolecules* **2007**, *8*, 3860−3870.
(24) Noordover, B. A. J.; van Staalduinen, V. G.; Duchateau, R.; Koning, C. E.; van Benthem, R. T. A. M.; Mak, M.; Heise, A.; Frissen, A. E.; van Haveren, J. *Biomacromolecules* **2006**, *7*, 3406−3416.
(25) Carothers, W. H. *J. Am. Chem. Soc.* **1929**, *51*, 2548−2559.
(26) Wang, Z.; Zhang, X.; Wang, R.; Kang, H.; Qiao, B.; Ma, J.; Zhang, L.; Wang, H. *Macromolecules* **2012**, *45*, 9010−9019.
(27) Zhao, H. P.; Zhang, J. F.; Sun, X. S.; Hua, D. H. *J. Appl. Polym. Sci.* **2008**, *110*, 647−656.
(28) Sharma, V.; Kundu, P. P. *Prog. Polym. Sci.* **2008**, *33*, 1199−1215.
(29) Overeem, A.; Buisman, G. J. H.; Derksen, J. T. P.; Cuperus, F. P.; Molhoek, L.; Grisnich, W.; Goemans, C. *Ind. Crops Prod.* **1999**, *10*, 157−165.
(30) Buisman, G. J. H.; Overeem, A.; Cuperus, F. P. In *Recent developments in the synthesis of fatty Acid Derivatives*; Knothe, G., Derksen, J. T. P., Eds.; AOCS Press: Champaign, IL, 1999; Chap. 8, pp128−140.
(31) Noordover, B. A. J.; Heise, A.; Malanowksi, P.; Senatore, D.; Mak, M.; Molhoek, L.; Duchateau, R.; Koning, C. E.; van Benthem, R. A. T. M. *Prog. Org. Coat.* **2009**, *65*, 187−196.
(32) Baye, T.; Becker, H. C.; Witzke-Ehbrecht, S. *Ind. Crops Prod.* **2005**, *21*, 257−261.
(33) Thompson, A. E.; Dierig, D. A.; Kleiman, R. *Ind. Crops Prod.* **1994**, *2*, 299−305.
(34) Flory, P. J. *Principles of Polymer Chemistry*; Cornell University Press: Ithaca, NY, 1953.
(35) Blank, W. T.; He, Z. A.; Picci, M. *J. Coat. Technol.* **2002**, *926*, 33−41.
(36) Halley, P. J.; George, G. A. *Chemorheology of Polymers: From Fundamental Principles to Reactive Processing*; Cambridge University Press: New York, 2011.
(37) Urayama, K.; Miki, T.; Takigawa, T.; Kohjiya, S. *Chem. Mater.* **2004**, *16*, 173−178.
(38) Deplace, F.; Carelli, C.; Langenfeld, A.; Rabjohns, M. A.; Foster, A. B.; Lovell, P. A.; Creton, C. *ACS Appl. Mater. Inter.* **2009**, *1*, 2021−2029.
(39) Udagama, R.; Degrandi-Contraires, E.; Creton, C.; Graillat, C.; McKenna, T. F. L.; Bourgeat-Lami, E. *Macromolecules* **2011**, *44*, 2632−2642.
(40) Aitziber Lopez, A.; Degrandi-Contraires, E.; Canetta, E.; Creton, C.; Keddie, J. L.; Asua, J. M. *Langmuir* **2011**, *27*, 3878−3888.
(41) Winter, H. H.; Chambon, F. *J. Rheol.* **1986**, *30*, 367−382.
(42) Dusek, K.; Prins, W. *Adv. Polym. Sci.* **1969**, *6*, 1−102.
(43) Stockmayer, W. H. *J. Chem. Phys.* **1943**, *11*, 45−55.
(44) Patel, S. K.; Malone, S.; Cohen, C.; Gillmor, J. R.; Colby, R. H. *Macromolecules* **1992**, *25*, 5241−5251.
(45) Urayama, K.; Kohjiya, S. *J. Chem. Phys.* **1996**, *104*, 3352−3359.
(46) Chambon, F.; Winter, H. H. *J. Rheol.* **1987**, *31*, 683−697.
(47) Winter, H. H.; Morganelli, P.; Chambon, F. *Macromolecules* **1988**, *21*, 532−535.
(48) Ferry, J. D. *Viscoelastic Properties of Polymers*, 3rd ed.; John Wiley & Sons: New York, 1980; Vol. *1*.
(49) Neugebauer, D.; Zhang, Y.; Pakula, T.; Sheiko, S. S.; Matyjaszewski, K. *Macromolecules* **2003**, *36*, 6746−6755.
(50) Zhang, Y.; Chung, I. S.; Huang, J.; Matyjaszewski, K.; Pakula, T. *Macromol. Chem. Phys.* **2005**, *206*, 33−42.
(51) Dahlquist, C. A. *Adhes. Age* **1959**, *2*, 25.
(52) Zosel, A. *J. Adhes.* **1991**, *34*, 201−209.
(53) Erman, B.; Mark, J. E. *Structures and Properties of Rubberlike Networks*; Oxford University Press: New York, 1997.
(54) Lee, I.; Wool, R. P. *J. Polym. Sci., Part B: Polym. Phys.* **2002**, *40*, 2343−2353.
(55) Zhang, B. M.; Chaudury, M. K.; Brown, H. R. *Science* **1995**, *269*, 1407−1409.
(56) Feldstein, M. M.; Siegel, R. A. *J. Polym. Sci., Part B: Polym. Phys.* **2012**, *50*, 739−772.
(57) Carelli, C.; Deplace, F.; Boissonnet, L.; Creton, C. *J. Adhes.* **2007**, *83*, 491−505.
(58) Shin, J.; Martello, M. T.; Shrestha, M.; Wissinger, J. E.; Tolman, W. B.; Hillmyer, M. A. *Macromolecules* **2011**, *44*, 87−94.
(59) Pu, G.; Dubay, M. R.; Zhang, J.; Severtson, S. J. *Ind. Eng. Chem. Res.* **2012**, *51*, 12145−12149.
(60) Bowman, H.; Hudson, B. W.; patent WO/2012/030819.
(61) Doi, Y. F., Fukuda, K., *Biodegradable Plastics and Polymers*; Elsevier: Amsterdam, 1994.
(62) Albertsson, A. C.; Varma, I. K. *Adv. Polym. Sci.* **2002**, *157*, 1−179.